Arab J Sci Eng (2014) 39:311–324
DOI 10.1007/s13369-013-0850-4

RESEARCH ARTICLE - EARTH SCIENCES

Sediment Composition and Provenance of the Pab Formation, Kirthar Fold Belt, Pakistan: Signatures of Hot Spot Volcanism, Source Area Weathering, and Paleogeography on the Western Passive Margin of the Indian Plate During the Late Cretaceous

Muhammad Umar · Henrik Friis · Abdul Salam Khan · Gilbert Kelling · Akhtar Muhammad Kassi · Muhammad Amjad Sabir · Muhammad Farooq

Received: 27 July 2012 / Accepted: 15 February 2013 / Published online: 7 November 2013

Abstract Petrographic and geochemical data collected from the Pab Formation, a late Cretaceous clastic sequence exposed in the Kirthar Range of western Pakistan, yield important clues about the influence of the varied source regimes, transportation routes and volcanic input that have influenced the composition of sediments comprising this formation. Detrital compositional modes, petrotectonic discrimination diagrams and paleocurrent data all demonstrate that the Pab sands were ultimately derived from granitic–gneissic terranes forming the Indian Craton, exposed to the E and SE of the study area, with probable supplementary contribution from the mature, ancient sedimentary cover of the craton. These data also confirm that the two contemporaneous depositional systems operating during accumulation of the Pab Formation in this area were supplied from somewhat different sources and through different routes. Sediments deposited in the Central Kirthar sub-basin were derived from the East, while coeval deposits within the Southern Kirthar sub-basin were supplied from SSE and include relatively fresh volcanic detritus that is interpreted as the product of the major Deccan Trap volcanic episode, initiated during late Maastrichtian times. Moreover, geochemical indicators demonstrate that the ultimate composition of Pab sediments has been strongly influenced by intense chemical weathering, associated with warm/humid climatic conditions in the source areas, accompanied by significant diagenetic effects.

Keywords Sediment composition · Provenance · Weathering · Paleoclimate · Hot spot volcanism · Diagenesis

الخلاصة

تُعطي البيانات الصخرية والجيوكيميائية التي تم جمعها من تشكيل PAB، في التسلسل التفكيكي الطباشيري المتأخر والمكشوفة في نطاق كيرثار غرب باكستان مؤشرات هامة حول تأثير أنظمة المصدر المتنوعة، وطرق النقل والمدخلات البركانية التي أثرت في تكوين الرواسب التي يتألف منها هذا التشكيل. إن الأنماط التركيبية الفتاتية، ورسوم هيكلية البترول البيانية التمييزية، وبيانات مسارات المياه تثبت جميعا أن رمالPAB قد استمدت في نهاية المطاف من التضاريس الأرضية الجرانيتية ـ صواني التي شكلت طبقة كراتون الهندية، والمكشوفة لمنطقة الدراسة E وSE، مع مساهمة تكميلية محتملة من غلاف الرواسب القديمة الناضجة لطبقة الكراتون. وتؤكد هذه البيانات أيضا أن اثنين من أنظمة الترسيب المعاصرة العاملة خلال تراكم تشكيل PAB في هذه المنطقة تم تزويدها من مصادر مختلفة إلى حد ما، ومن خلال طرق مختلفة. وقد اشتقت الرواسب المودعة في وسط حوض كيرثار الفرعي من الشرق، في حين تم تزويد الودائع المعاصرة في حوض كيرثار الجنوبي الفرعي من SSE وتشمل نسبيا المخلفات البركانية الجديدة التي يتم تفسيرها على أنها نتاج مصيدة حادثة ديكان البركانية الكبرى، المتولدة خلال أواخر أوقات العصر الطباشيري. علاوة على ذلك تُثبت المؤشرات الجيوكيميائية أن التكوين النهائي لرواسب PAB قد تأثر بشدة بالعوامل الجوية الكيميائية المكثفة، ويرتبط مع الظروف المناخية الحارة / الرطبة في مناطق المصدر، مصحوبا بآثار النشأة المتأخرة الكبيرة.

M. Umar (✉) · M. A. Sabir · M. Farooq
Department of Earth Sciences, COMSATS Institute of Information Technology, Abbottabad, Pakistan
e-mail: umarkhan09@yahoo.com

H. Friis
Department of Geoscience, Aarhus University, Aarhus, Denmark

A. S. Khan
Centre of Excellence in Mineralogy, University of Balochistan, Quetta, Pakistan

G. Kelling
School of Physical and Geographical Sciences, University of Keele, Staffordshire, UK

A. M. Kassi · M. Umar
Department of Geology, University of Balochistan, Quetta, Pakistan

1 Introduction

Source-geology, paleoclimate, transport processes and distances and post-depositional changes are the main factors controlling the composition of sandstones [1,2]. Petrographic analysis is the standard method [3,4] used in the study of provenance, and a range of petrographic and geochemical techniques may be deployed to determine the provenance of detrital rocks for the purpose of reconstructing the paleogeography and paleotectonics of sedimentary basins [5]. Moreover, the relationship of detrital compositional modes with plate tectonic setting is well established and used both in modern and ancient systems [6], while depositional environments [7,8], diagenetic history [9] and climatic conditions [10] are further important factors influencing detrital modes.

Furthermore, petrographic analyses of detrital rocks are useful in the assessment of paleogeographic reconstructions [5], including the paleogeology [11] and nature of the weathering [12–14] of the source area. Again, studies of the provenance, tectonic settings and paleoclimatic regimes of ancient systems [14–16] as well as crustal evolution [17] can be greatly enhanced by determining the geochemical compositions of sedimentary rocks. The geochemical parameters and models such as K_2O/Al_2O_3 ratio, Index of Chemical Variability (ICV) [18], Chemical Index of Alteration (CIA) [19], $SiO_2-Al_2O_3+K_2O+Na_2O$ diagram [20] and $Al_2O_3-CaO + Na_2O-K_2O$ (A–CN–K) plot [21] all serve to emphasize the importance of provenance study, paleoclimate, maturity and weathering intensity [18,21].

Previous published studies concerning the Pab Formation in the Kirthar Fold Belt of southwestern Pakistan have presented the detailed sedimentology [22,23] and aspects of the diagenesis of these sediments [24]. However, there is little or no detailed information available on the petrology and geochemistry of the Pab sediments or their provenance. Thus, the study reported in this article focused on these compositional attributes of this Late Cretaceous formation, not least because the Pab represents the first great flush of coarse clastic sediment on to the western passive margin of the Indian Plate since its separation from the remainder of Gondwana in the early Mesozoic.

2 Geology and Depositional Framework

2.1 Geological Framework

The study area (Kirthar Fold Belt "KFB") [25] is situated near the western transform-faulted (Ornach Nal Fault) [26] margin of the Indian Plate and was formed as a result of Indian–Eurasian continental collision. The KFB links the Makran accretionary prism in the west with the main Himalayan collision zone to the north [25]. During the Cretaceous the Indian Plate rotated anticlockwise towards the north and Madagascar consequently separated from Indian Plate [27]. The Indian Plate also passed over the Reunion mantle hot spot during the Late Campanian–Maastrichtian [28], which caused episodes of uplift and erosion that were ultimately responsible for supplying the great volume of coarse detritus represented in the Pab Formation to basins on the submerged northern and western margins of the Indian Plate.

The KFB is dominated by sedimentary rocks, ranging in age from the Jurassic Ferozabad Group to the Dada Conglomerates of Pleistocene age (Table 1; Fig. 1). The Pab Formation comprises a thick sequence of alternating sandstones, mudstones and marls. The occurrence and thickness of marl beds decrease upward as they are gradually replaced by mudstone. The sandstones are moderate yellowish brown (10YR 5/4), light brownish grey (5YR 6/1), medium grey (N5), very light grey (N8), and pale red purple (5PR 6/2) in color. They are fine to very coarse-grained and locally pebbly. Mudstone is thin bedded, greenish grey, olive grey and mottled red; massive, fissile and bioturbated. The marls are moderate yellowish brown (10YR 5/4), brownish grey (5YR 4/1), pale yellowish brown (10YR 6/2) and greyish orange (10YR 7/4). They may be finely laminated, thin bedded, cleaved or massive. The upper and lower contacts of Pab Formation are conformable with the Ranikot Group and lower Mona Jhal Group [29], respectively. Based on the presence of *Orbitoides* (*Lepidorbitoides*), a late Cretaceous age is assigned to the Formation [29].

The Pab Formation was formed within at least two depositional basins, one of which is the Central Kirthar sub-basin (CKsb) and the other is the Southern Kirthar sub-basin (SKsb: Figs. 2, 3 and 4) [23]. In the CKsb, the Pab is characterized by shallow-marine (shelfal) deposits (Fig. 5a, b), some of which were the products of episodic storm waves and westward flowing, hyperpycnal flows of high density were produced at river mouths during catastrophic flooding conditions. Pab sediments found in the SKsb range from fluviodeltaic deposits (Fig. 5c, d) to deep marine clastic turbidites (Fig. 5e, f) [22,23].

Paleocurrent data collected from Pab sequences within these two sub-basins reveal a strong contrast in contemporary sediment transport paths: flows recorded from the spectrum of fluvial and marine shelf deposits represented in the Pab fill of the CKsb are almost exclusively E to W; however, Pab detritus was conveyed into the SKsb by currents that flowed broadly from S to N [22]. The existence of these two contrasting depositional systems is indicative of the complex physiography of the onshore sector of this margin (as evidenced by syn-sedimentary faulting and elevation of the paleo-Jacobabad High), together with the varied bathymetry of the adjacent sea floor. This complexity is attributable to Cretaceous tectonic activity which is known to have affected the western margin of the northwards-drifting Indian Plate [23].

Table 1 Generalized stratigraphy of the Kirthar Fold Belt, showing stratigraphic position of the Pab Formation and of the Deccan Trap Volcanics (after [29,38,39])

Age	Group/Formation		Lithology
Holocene	Recent–Subrecent		Mixture of clay, sand and gravel
Unconformity			
Pleistocene	Dada Conglomerates		Boulders and pebble conglomerates with subordinate coarse-grained sandstone
Pliocene	Manchar Formation		Interbedded sandstone and shale with subordinate conglomerate
Unconformity			
Miocene	Gaj Formation		Shale, sandstone with subordinate limestone and conglomerate
Oligocene	Nari Formation		Sandstone interbedded with shale
Eocene	Kirthar Formation		Fossilifereous limestone interbedded with shale
	Ghazij Formation		Dominantly shale with minor sandstone
Paleocene	Rani Kot Group	Age of Deccan Trap Volcanism	Intraclastic limestone and shale
Maastrichtian-	Pab Formation		Sandstone intercalated with mudstone and marl
Early–Late Cretaceous	Mona Jhal Group		Marl, arenaceous limestone, micritic limestone with shale, siltstone
Disconformity			
Early–Late Jurassic	Ferozabad Group		Limestone interbedded with shale and marl

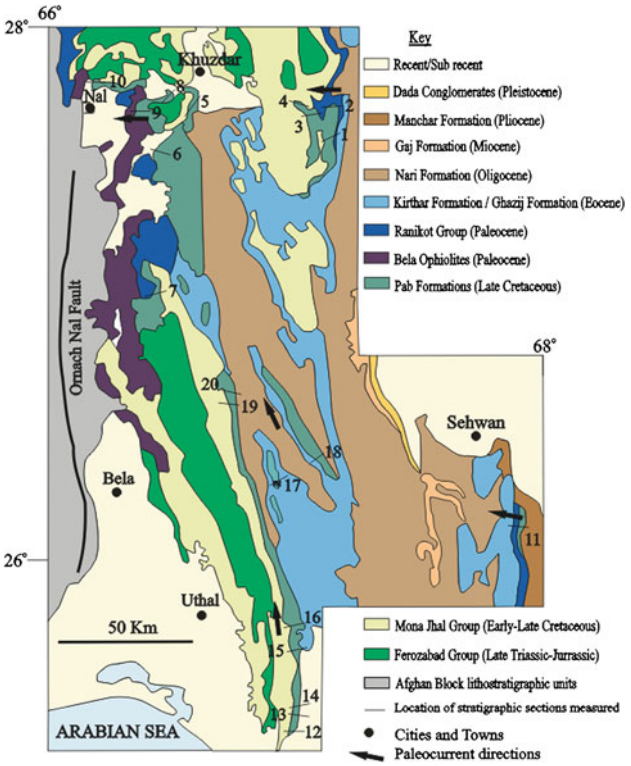

Fig. 1 Generalised geological map of the Kirthar Range, southwest Pakistan showing location of the 20 measured sections in the Pab Formation [after [23]]. The boundary between the Central Kirthat sub-basin (CKsb) and the South Kirthar sub-basin (SKsb) falls between sections 11 and 20

Within the Pab sequence the overall thickening- and coarsening-upwards trend, the frequency of hummocky bedforms and vertical facies variations all indicate that these late Cretaceous sediments were formed during a broadly regressive phase. Sandstone compositions and the observed paleocurrent directions (Fig. 2) demonstrate that the detritus forming the Pab was supplied through different routes and from different sectors of the Indian Craton, located E and SE of the study area.

2.2 Methodology

Samples of sandstone and mudstone were collected from 20 stratigraphic sections measured through the Pab Formation within both the Central and Southern Kirthar sub-basins (Fig. 1). An Olympus BH-2 Modal microscope was used to examine a total of 65 thin sections of sandstones, taken from almost all the sampled sequences. To reduce grain-size effects and ensure optimum coverage of samples, 500 points were counted in all thin sections, using the Gazzi Dickinson method [30]. Point counting data of sandstone samples have been plotted in triangular diagrams (Q–F–L; Qm–F–Lt and Qp–Lv–Ls) [3,4] to facilitate identification of provenance. A Shimadzu Rayny EDX-700 HS X-Ray fluorescence spectrometer was used for geochemical analyses of mudstone and sandstone samples. Carbon coating of polished thin sections was carried out by means of a Leica Emitech K950 Evaporator, while gold coating of sandstone chips for

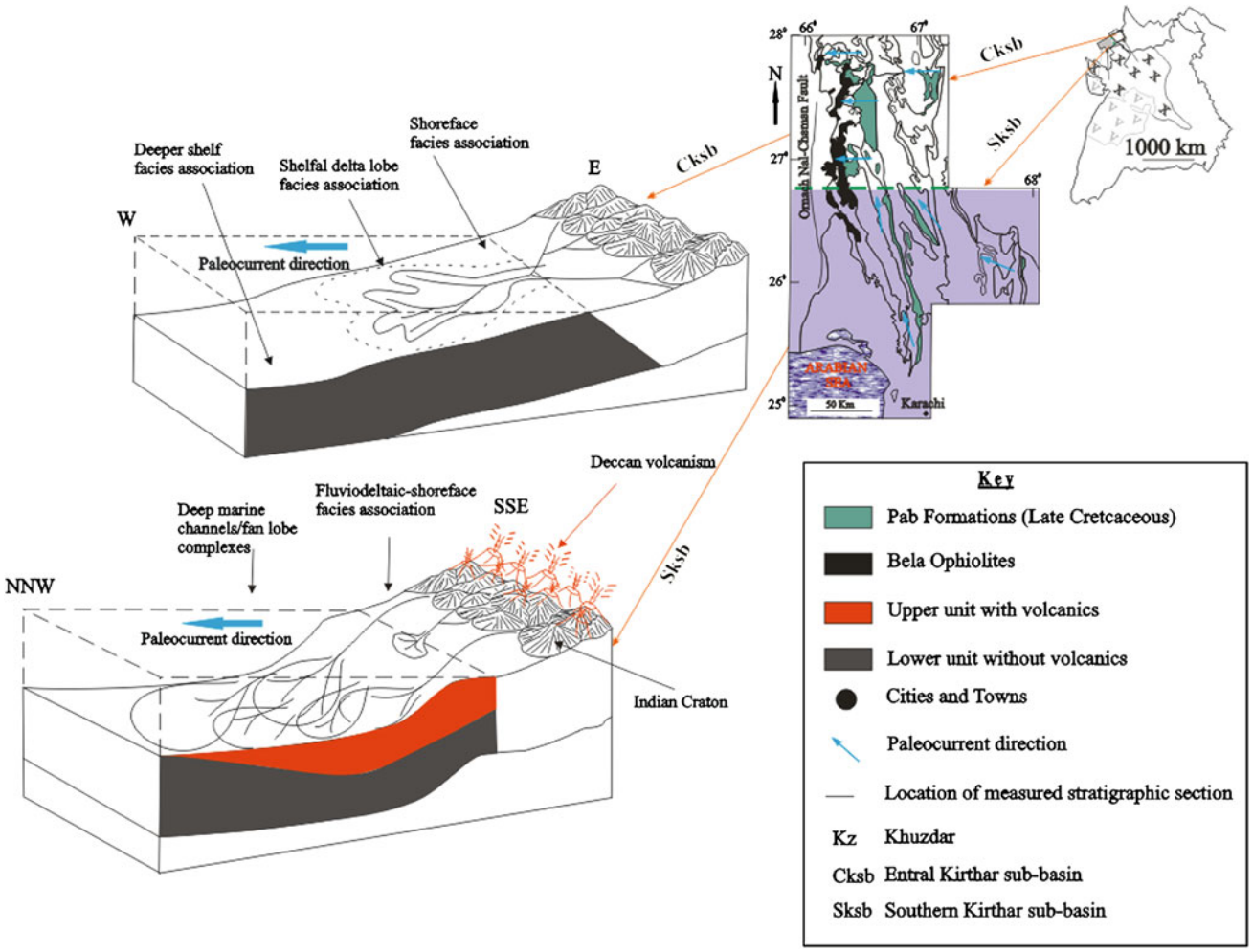

Fig. 2 Schematic showing (i) *top right* position of the Indian Plate during the Late Cretaceous (*X*s show the north Indian craton; *V*s denote Deccan Traps province) and location of the study area, with accompanying enlarged geological sketch showing positions of the CKsb and SKsb sub-basins; (ii) *left side* paleogeographical sketch-diagrams illustrating depositional settings, aggregate paleoflow directions (*blue arrows*) and source terranes for Pab deposits in the Central and Southern Kirthar sub-basins, respectively. Note volcanic input (*dark yellow*) in the Pab fill of the SKsb during later stages of Pab deposition

Scanning electron microscopy (SEM) studies was undertaken. A Jeol JSM 6400 machine, equipped with EDAX, was used for SEM. The paleoflow data reported below was recorded during fieldwork, from flutes, grooves and cross bedding and has been corrected for tectonic rotation.

3 Results and Discussion

3.1 General Results

Our petrographic study shows that Pab sandstones are medium to very coarse grained (locally pebbly), moderately to well sorted, and are dominated by subrounded to well-rounded grains. Thus, these arenites are defined as texturally submature to supermature. The average composition of the sandstones sampled in each measured section is shown in Table 2. Quartz is the most abundant constituent, ranging in abundance from 59.5 to 87.4 %. Monocrystalline quartz (Fig. 6a) is dominant and ranges from 56.7 to 84.2 %, whereas polycrystalline quartz is the subordinate variety (0.1–8.2 %). Feldspar forms a minor constituent of these sandstones throughout all the sampled sections (0.2–1.4 %; Fig. 6b, c). Plagioclase (Fig. 6d) is less common than K-feldspar and is present in only trace amounts in a few samples. Sedimentary rock fragments constitute up to 3.13 % and are mainly composed of chert, but siltstone fragments (Fig. 6e) are observed as a smaller fraction. Rock fragments of volcanic origin (mainly basaltic) are restricted to the SKsb, where they are frequent in the upper portion of the Pab Formation. Overall, the content of volcanic rock fragments (Fig. 6f) ranges from 2.1 to 18.3 % and their frequency increases stratigraphically

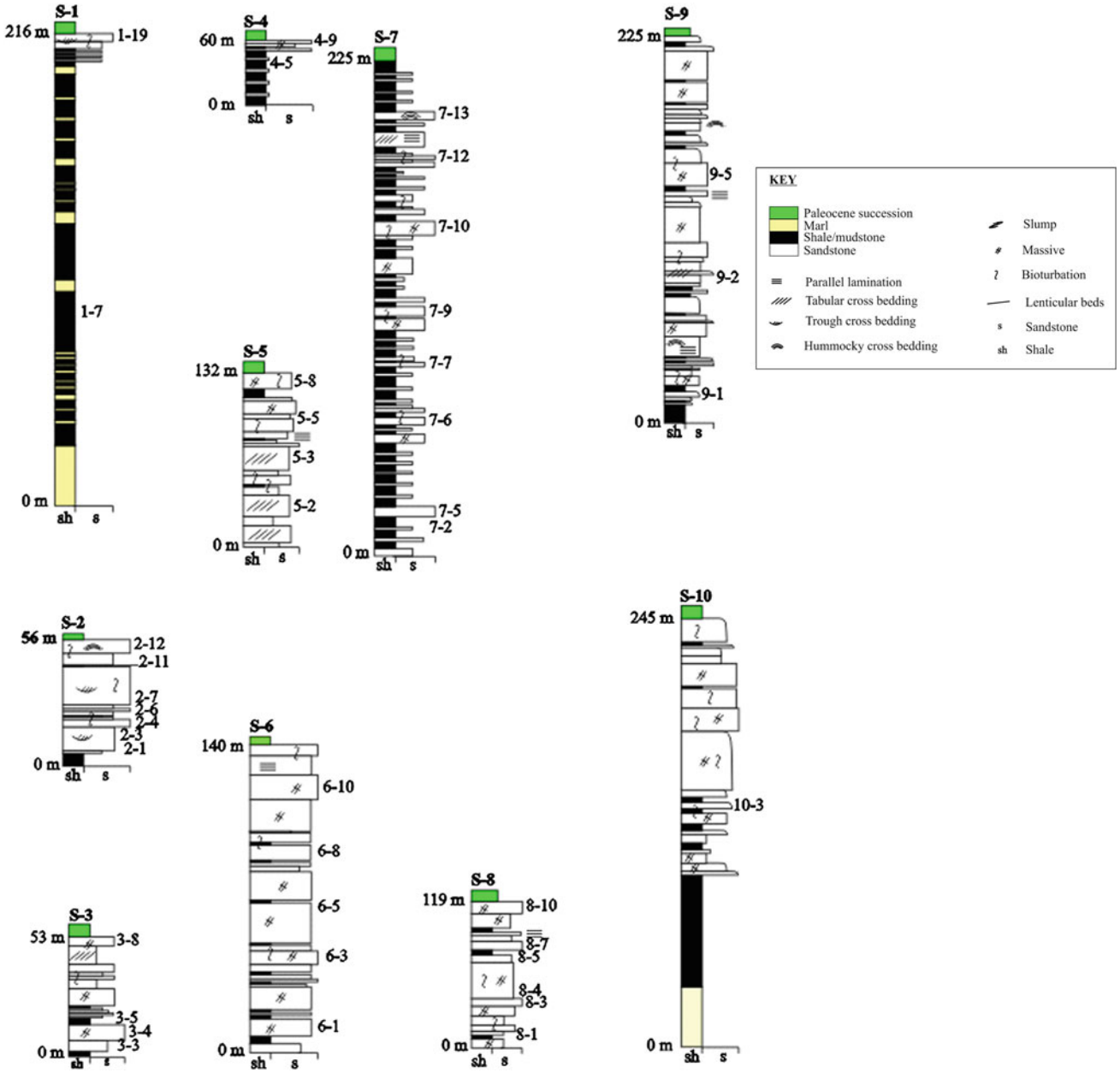

Fig. 3 Measured stratigraphic sections (S-1 to S-10) in CKsb, showing positions of samples analyzed and the lithological characters of the shoreface-delta lobe-shelf ramp depositional facies of the Pab Formation in this sector of the Kirthar Belt (modified after [22,23])

upwards and decreases slightly towards distal depositional settings.

With respect to geographical distribution, the micrometric data show that the Pab sandstones in the CKsb successions and in most of the SKsb sections are dominated by quartz (maximum = 99.77 %), with very subordinate feldspar (maximum = 4.61 %) and rare sedimentary lithic fragments (0.54 %, excluding chert). Significant percentages of volcanic fragments (maximum = 29.74 %) are present only in sandstones from the uppermost levels of the Pab in the SKsb. In addition, trace amounts of mica are recorded in most samples. These framework grains are separated by generally less abundant cementing minerals (calcite, quartz and iron oxide/hydroxide are common).

The content and distribution of major elements in the Pab sandstones confirms the mineralogical composition of the samples studied. The main geochemical constituent of these sandstones is SiO_2 (92.02–98.06 %), followed by CaO, Fe_2O_3 and K_2O (3.26, 2.98 and 1.71 % respectively: see Table 3). The sandstones contain trace amounts of ZrO_2, V_2O_5, MnO, Cr_2O_3, ZnO, NiO and SrO. In the mudstone samples the major oxides (Table 4) are Al_2O_3, SiO_2, Fe_2O_3,

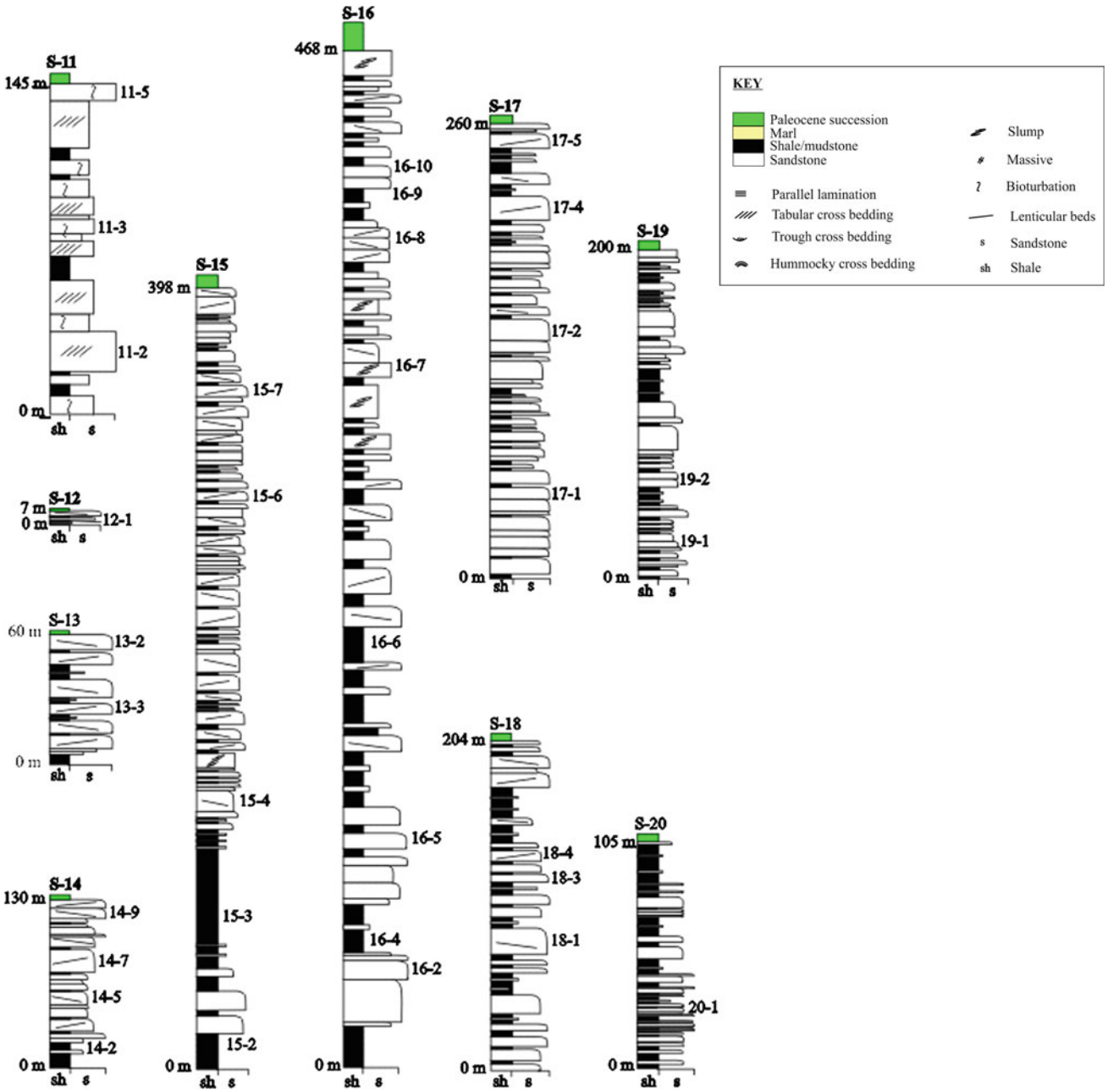

Fig. 4 Stratigraphic sections (S-11 to S-20) measured in SKsb, showing positions of analyzed samples and the lithological characters of the fluviodeltaic-deep marine facies of the Pab Formation in this sector of the Kirthar Belt (modified after [23]). *S* on top of each log means Section measured

K_2O and CaO, whereas TiO_2, MnO, SrO, ZrO, V_2O_5, Nb_2O, Rb_2O and ZnO represent the minor oxides fraction.

Provenance studies of sand-sized sediments in ancient sedimentary systems can be rendered difficult because of source material modifications through processes such as weathering, erosion, transport and deposition and also by post-depositional processes, such as diagenesis [31]. Specifically, the mineralogical maturity of a sediment may be strongly influenced by the nature and duration of chemical and physical weathering processes that the detrital components have undergone [32,33]. For instance, the extent of feldspar conversion to secondary clay minerals is related to paleoclimate and degree of paleoweathering [33], along with tectonism [34].

In this context the sedimentological, petrographic and geochemical results obtained from the Pab Formation sand-

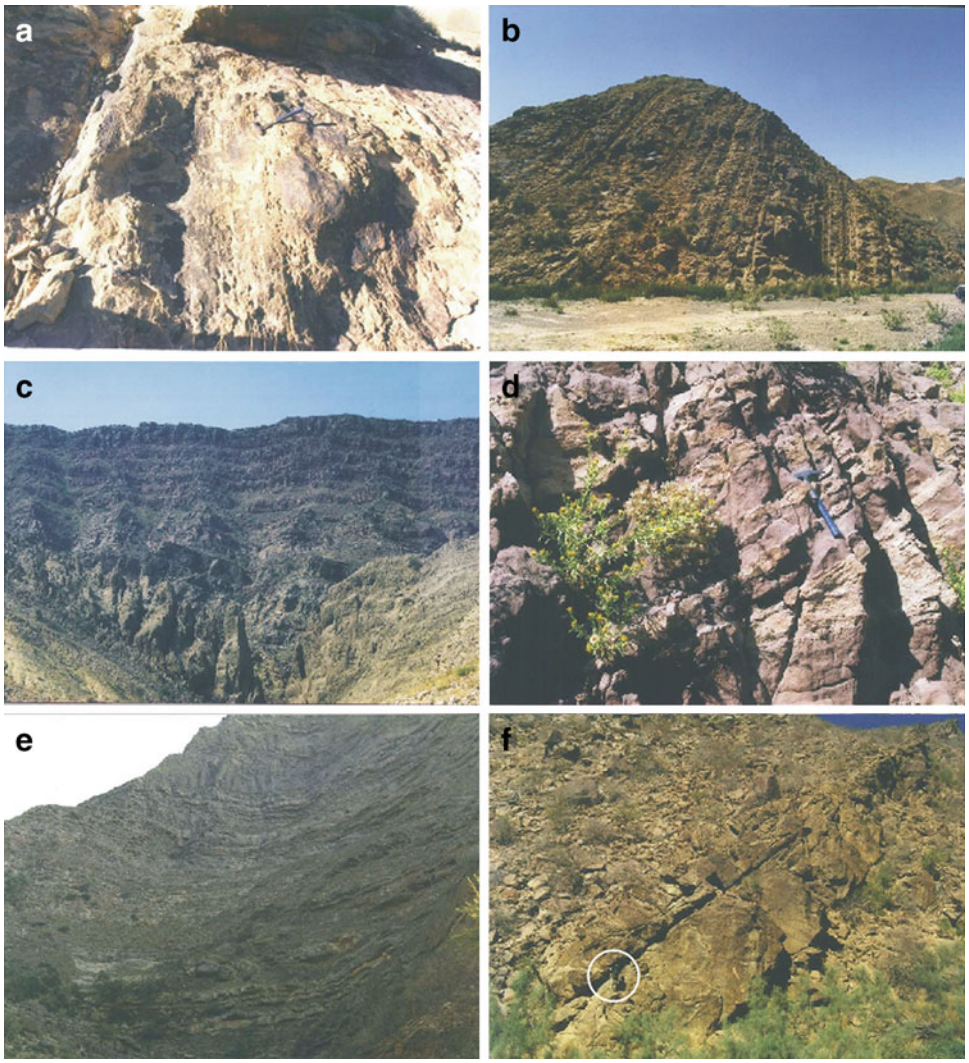

Fig. 5 Field photographs showing general views and dominant facies identified within the outcropping Pab in the Kirthar region (**a**, **b** shelfal delta lobe sand-bodies; **c**, **d** fluviodeltaic sandstone-mudstone bodies; **e**, **f** deep marine channel sands and submarine fan lobes)

stones reveal that several factors have influenced their provenance, notably the evolving paleogeography and morphology of the western Indian passive margin, the nature and orientation of sediment-transporting paleoflows, and the nature and rates of chemical weathering of labile grains in the source areas. An additional important local factor is the inception, nature and duration of latest Mesozoic (Deccan Trap) volcanism, hosted on the western Indian craton. The complex topography/bathymetry of the western Indian continental margin during the late Cretaceous is a significant factor, since this is considered to be responsible for the creation of the two coeval depositional systems considered here and also for generation of two distinct paleoflow patterns (sediment-supply routes) associated with the two sub-basins, as described in Sect. 2.1, above [23].

A further major difference in the composition of sandstones from these two sub-basins is the occurrence of volcanic clasts in the upper levels of the SKsb fill. While Pab sandstones in the CKsb and in the lower part of the SKsb fill-sequence are almost exclusively mature quartz-arenites in composition, sandstones from the stratigraphically highest horizons in the SKsb are more lithic in nature and contain appreciable percentages of volcanic (basaltic) fragments (Table 2; Figs. 2, 6c, f).

3.2 Petrotectonic Classification of Pab Sandstones

Triangular plots of Q–F–L and Qm–F–Lt [3,4] indicate that most of the sandy detritus forming the Pab Formation was supplied from Craton Interior, Recycled Orogen and Quartzose Recycled settings (Fig. 7a, b). However, sandstones in the upper levels of the SKsb fill were derived from Arc Orogen as well as Craton Interior settings (Fig. 7a, c) [3,4]. Taken with the predominance of quartz in these sandstones and the prevalence of tourmaline and zircon in heavy mineral suites, these plots demonstrate that the bulk of the Pab detritus originated through recycling from plutonic felsic, metamorphic or mature sedimentary cover sources [35]. Moreover, the local

Table 2 Average point counting data of Pab sandstones from measured stratigraphic sections in CKsb and SKsb

Section no.	*n*	Qtzm	Qtzp	Qtz	*F*	Lv	Ls	Cal	Ioc	Clay	QtzO	Hm	Clay + F	Clay + Lv	Sub-basin
1	1	74.2	4.4	78.6	0.2	0	0.6	0	3	4.8	12.4	0.4	5	4.8	CKsb
2	6	78.76	2.16	80.92	1.23	0	2.3	0	0.96	3	10.56	0.66	4.23	3	CKsb
3	3	73.73	0.8	74.53	0.73	0	3.13	0	13	3.73	4.2	0.66	4.46	3.73	CKsb
4	1	74.4	0.6	75	1.4	0	0	0	18.8	1.2	2.6	1	2.6	1.2	CKsb
5	4	72.95	0.1	73.05	1.3	0	0.4	20	0	2.15	2.85	0.25	3.45	2.15	CKsb
6	5	75.2	0.64	75.84	0.56	0	1.2	17.24	0.04	1.6	3.48	0.04	2.16	1.6	CKsb
7	7	74.05	0.68	74.73	0.71	0	0.22	20.42	0.42	1.37	1.97	0.11	2.08	1.37	CKsb
8	6	72.56	8.4	80.96	0.5	0	0.7	19.4	2.03	1.86	1.93	0.16	2.36	1.86	CKsb
9	3	62.6	4.06	66.66	0.4	0	0.6	25.66	0	4.86	1.26	0.53	5.26	4.86	CKsb
10	1	70.6	5.8	76.4	0.8	0	1.2	9.82	3.4	2.4	4.6	1.4	3.2	2.4	CKsb
11	3	56.7	2.8	59.5	0.5	0	0.5	12.8	22.6	1.8	2	0.3	2.3	1.8	SKsb
11	1	66.2	0.8	67	0.6	17.6	0	10.6	1.2	1.2	1.8	0	1.8	18.8	SKsb
13	2	73.8	0.8	74.6	0.2	8.9	0.1	11.8	0	0.8	3.6	0	1	9.7	SKsb
14	3	68	1.46	69.46	0.4	9.4	0.33	16.4	1.13	1.6	1.26	0	2	11	SKsb
15	1	84.2	3.2	87.4	0.4	0	0	7.2	1.4	1.2	2.4	0	1.6	1.2	SKsb
15	2	71.9	0.2	72.1	1.1	18.3	0.1	2.6	1.1	0.3	4.4	0	1.4	18.6	SKsb
16	2	73.7	2.2	75.9	0.5	0	0.3	14.1	2.6	3.4	2.9	0.3	3.9	3.4	SKsb
16	3	67.4	0.26	67.66	1.13	7.73	0	17.66	0.46	1.86	3.46	0	2.99	9.59	SKsb
17	2	74.7	1.6	76.3	0.3	0	0.5	14.5	0.9	2	4.8	0.7	2.3	2	SKsb
17	2	79.7	0.2	79.9	0.7	2.1	0	9.6	0.2	1.7	5.1	0.4	2.4	3.8	SKsb
18	1	83	4.8	87.8	0.4	0	1.2	0	1.2	6.6	1.8	1	7	6.6	SKsb
18	2	76.5	0.6	77.1	0.7	2.6	0.3	14.9	0	1.2	2.7	0.5	1.9	3.8	SKsb
19	2	79.8	4.3	84.1	0.2	0	0.4	6.6	0	3.8	3.8	1.1	4	3.8	SKsb
20	2	71.6	5.4	77	0.3	0	0	15.3	0.2	2.3	4.5	0.4	2.6	2.3	SKsb

n number of samples from relevant stratigraphic section; *Qtzm* monocrystalline quartz; *Qtzp* polycrystalline quartz; *Qtz* total quartz; *F* total Feldspar; *Lv* volcanic clasts; *Ls* sedimentary rock fragments, including chert; *Cal* calcite; *Ioc* iron oxide/hydroxide; *clay* clay minerals (mainly diagenetic); *QtzO* quartz overgrowths; *Hm* heavy minerals

occurrence of volcanic clasts strongly suggests that this recycling was induced by uplift of older (cratonic) rocks as a result of magmatism (arc volcanism), rather than through purely tectonic processes.

Stratigraphically, there is little change in the composition of the Pab sands in either sub-basins, other than the introduction of basaltic fragments in the upper horizons of the SKsb (up to 29.74 % of the detrital grains). Moreover, transport directions (while different between the sub-basins: see Sect. 2.1 above) remained essentially constant throughout deposition of the Formation [23]. These observations confirm that during the relevant span of geological time there was no significant change in the nature and location of the source regimes or the transport systems supplying the Pab detritus, apart from the addition of fresh volcanic debris to the detritus entering the SKsb in the later stages of its evolution.

In summary, paleocurrent data, petrography and geochemistry are consistent in demonstrating that the sediments of Pab Formation in SKsb sector were mainly sourced from the Indian Craton, now located E and SSE of the Kirthar Range (Fig. 2). Pab sediment deposited within the CKsb was transported westwards from more easterly sectors of the Craton (Fig. 2). Coeval sediments within the SKsb were initially supplied from lithologically similar Craton Interior terranes located SSE of this sub-basin. However, during deposition of the upper levels of the Pab significant volumes of volcanic (basaltic) detritus were supplied to this basin. This igneous material is attributed to the episode of volcanism, manifested in the Deccan Traps. This episode is widely ascribed to the passing of the western Indian Plate, during its northwards drift, over the Reunion mantle plume (hot spot) [28]. This latest Maastrichtian event is also believed to be responsible for the inception of India-Seychelles rifting [36].

Dating the eruption of the Deccan lava-pile thus assumes the importance in terms both of Indian plate motion and in refining the chronostratigaphic age of the Pab Formation. Biostratigraphic ages for sediments above and below the onshore Deccan basalts range from 68 to 69 Ma [37], whereas ^{40}Ar–^{39}Ar dates cluster between 63 and 69 Ma [38]. Paleo-

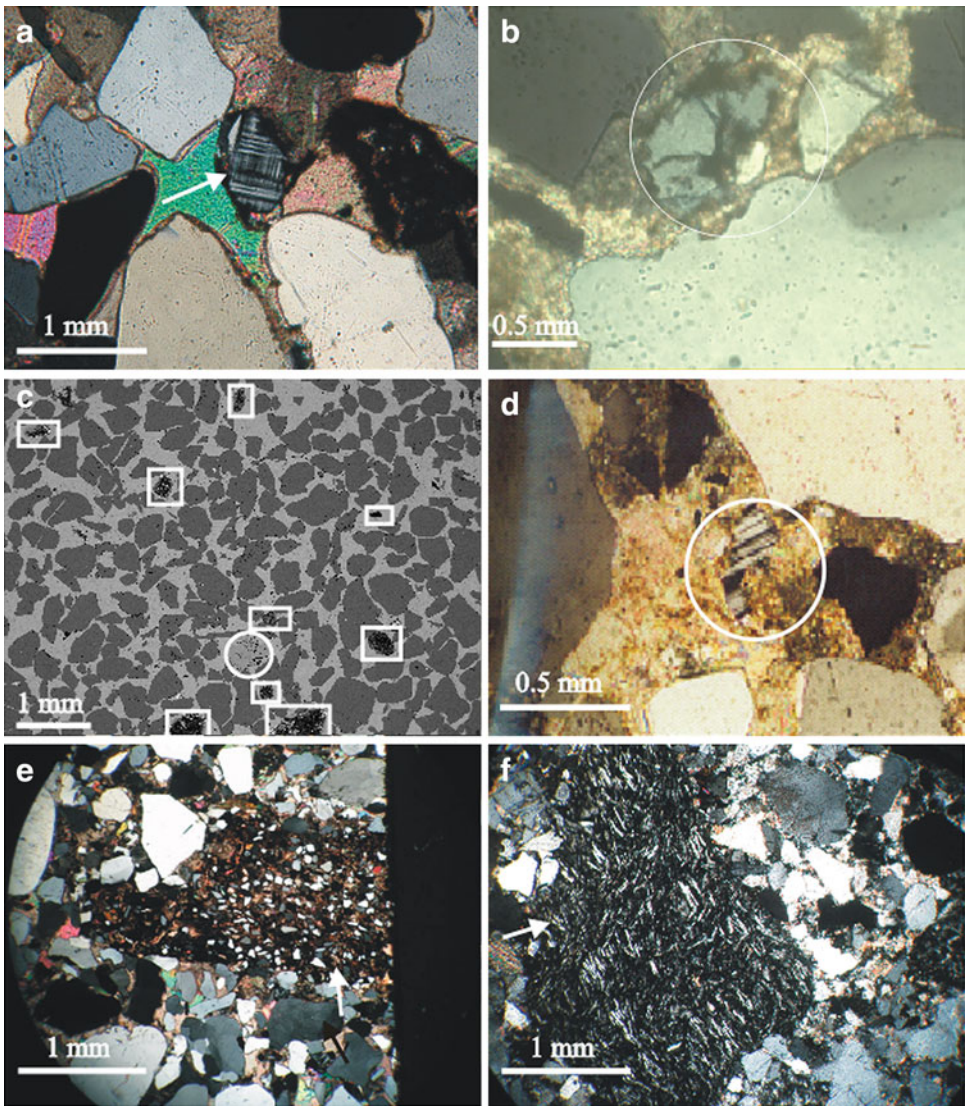

Fig. 6 Photomicrographs and SEM image of sandstones showing varieties of framework grains; **a** grains of monocrystalline nonundulose quartz and well-rounded microcline (*arrow*). **b** Altered orthoclase grain (*encircled*). **c** SEM image of a well-sorted sandstone sample, dominated by quartz grains (*dark grey*) with subordinate volcanic fragments (*in boxes*) and a single feldspar grain (*in circle*). **d** Plagioclase grain largely replaced by diagenetic calcite. **e** Clast of sedimentary rock (siltstone)—(*arrowed*). **f** *Arrow* shows volcanic clast (basaltic, with felted feldspar crystals) from sandstone in topmost horizons of SKsb

magnetic data from the lavas show three reversals (n–r–n), but 80 % display reversed polarity and are assigned to chron 29r (64.75–65.58 Ma) [39]. Our petrographic results show that Deccan basalts formed part of the detrital supply to the Pab Formation during the later stages of its deposition in the SKsb, probably soon after eruption of the lavas, showing that the top of the Pab is no older than ca. 65 Ma.

Finally, the absence of Deccan detritus from the Pab fill of the CKsb confirms that there was no significant Maastrichtian volcanic activity in the more easterly sectors of the Indian Craton.

3.3 Chemical Weathering in Pab Source and Sediment

A low feldspar content is characteristic of the Pab sandstones throughout the study area (Table 2; Figs. 6c, 7a, b). This was most probably caused by factors such as derivation from feldspar-poor source rocks or removal of feldspar through source-rock weathering, during transport, through post-depositional diagenesis or by a combination of these factors.

Geochemical data and related parameters from mudstones and sandstones provide clues that explain deficiencies in the feldspar content of sediments. For example, in mudstones the K_2O/Al_2O_3 ratios reflect the relative abundance of K-feldspar over plagioclase and clays. The K_2O/Al_2O_3 values range between 0.4 and 1 for K-feldspar and approximately 0.0–0.3 for clays. K_2O/Al_2O_3 ratios greater than 0.5 signify a significant original K-feldspar content, while ratios <0.4 indicate a relatively low amount [18]. The K_2O/Al_2O_3 ratios determined from the Pab mudstones in our study area range from 0.04 to 0.118, with an average value of 0.079, which are close to minimal values for K-feldspar in mudstone (Table 4).

With respect to Pab sandstones, the plot of SiO_2 versus $Al_2O_3 + K_2O + Na_2O$ [20], shown in Fig. 8a, the distribution

Table 3 Major and minor oxide contents of sandstones from the Pab Formation

Oxides/sample no.	Central Kirthar sub-basin (CKsb)				Southern Kirthar sub-basin (SKsb)						
	6–7	7–10	9–5	10–3	15–4	16–5	17–1	17–4	18–1	19–2	20–1
SiO_2	95.138	96.815	92.032	96.71	97.351	98.065	96.645	97.433	92.024	96.936	94.756
Fe_2O_3	0.691	0.361	2.871	1.257	0.306	0.65	1.343	0.316	2.983	0.397	0.753
CaO	3.169	0.497	2.219	0.54	1.352	0.518	0.522	1.48	2.224	0.547	3.266
K_2O	0.479	1.698	1.37	1.008	0.56	0.51	1.018	0.552	1.5	1.716	0.528
TiO_2	0.097	0.352	0.693	0.351	0.096	0.122	0.387	0.098	0.712	0.347	0.165
NiO	0	0	0	0	0	0.031	0	0	0	0	0
CuO	0	0.2	0	0	0.004	0.012	0	0.005	0	0.18	0
MnO	0	0	0.046	0	0	0	0	0	0.05	0	0
V_2O_5	0	0.031	0	0.006	0	0	0.007	0	0	0.029	0
SO_3	0	0.003	0.067	0.069	0.039	0.089	0.073	0.046	0.074	0.003	0
ZrO_2	0.004	0	0.296	0.005	0.004	0.002	0.005	0.004	0.311	0	0.005
Cr_2O_3	0	0	0.137	0	0.063	0	0	0.06	0.122	0	0
ZnO	0	0.006	0	0	0.004	0	0	0.005	0	0.007	0
SrO	0.002	0	0	0	0	0	0	0	0	0	0.002

Table 4 Concentration of major elements and other geochemical parameters in *mudstones* from the Pab Formation

Sample no:	Central Kirthar sub-basin (CKsb)				Southern Kirthar sub-basin (SKsb)							
	S1–7	S2–11	S3–5	S7–2	S12–1	S14–2	S15–1	S15–2	S15–3	S16–4	S16–6	S16–9
Oxides/Parameters												
SiO_2	43.45	40.22	48.45	46.58	42.88	32.91	40.34	42.25	40.23	44.07	43.84	43.37
Al_2O_3	41.96	45.9	39.44	44.32	44.82	46.05	45.97	49.23	47.8	44.65	49.46	49.32
CaO	5.314	4.92	2.858	0.31	1.975	2.013	0.68	0.803	4.768	2.288	0.252	0.458
Fe_2O_3	3.068	2.956	3.818	4.76	4.528	14.611	9.41	4.647	3.841	3.55	2.086	3.398
K_2O	4.972	5.414	4.528	3.21	4.638	2.941	2.16	2.372	2.619	4.994	3.856	2.901
TiO_2	0.409	0.496	0.712	0.74	1.053	0.895	1.01	0.642	0.471	0.397	0.459	0.398
MnO	0.034	0.037	0.121	0.045	0	0.517	0.32	0	0.229	0	0	0.106
V_2O_5	0.027	0.026	0.036	0	0.043	0.038	0.053	0.038	0.034	0.023	0.022	0.031
SrO	0.01	0.009	0.007	0	0.004	0.007	0.003	0.003	0.008	0.003	0.003	0.002
ZrO_2	0.008	0.007	0.007	0.007	0.008	0	0.005	0.004	0.005	0.004	0.005	0.003
Rb_2O	0.002	0.002	0.005	0.001	0.002	0.008	0	0	0.002	0.003	0.002	0.001
ZnO	0	0.005	0.007	0	0.006	0	0.008	0.005	0.005	0.002	0.003	0.004
NbO	0.001	0.001	0.001	0.001	0.002	0	0	0	0	0	0	0
CIA	80.31	81.62	84.22	92.64	87.14	96.16	94.18	93.94	86.61	85.97	92.33	93.62
ICV	0.32	0.075	0.30	0.13	0.22	0.44	0.24	0.17	0.24	0.25	0.13	0.14
CIW	88.76	90.32	93.24	99.30	95.78	95.81	98.54	98.39	90.93	95.12	99.49	99.08
K_2O/Al_2O_3	0.118	0.117	0.114	0.072	0.1	0.063	0.046	0.04	0.05	0.11	0.07	0.05

of datapoints suggests that humid environmental conditions prevailed in the source regime supplying the coarser Pab detritus.

Again, assessment of the mineralogy of the original detrital material represented in the mudstones is facilitated by use of the (ICV) index and the K_2O/Al_2O_3 ratio [18]. ICV is defined as below:

$$\mathrm{ICV} = (\mathrm{Fe_2O_3} + \mathrm{Na_2O} + \mathrm{CaO} + \mathrm{MgO} + \mathrm{Ti\,O_2}) / \mathrm{Al_2O_3}$$

Mature mudstones containing abundant clay minerals yield ICV values that are less than 1.0 [18]. Such mudstones are generally derived from volcanic terranes subject to intense weathering and only occasionally are they first cycle sed-

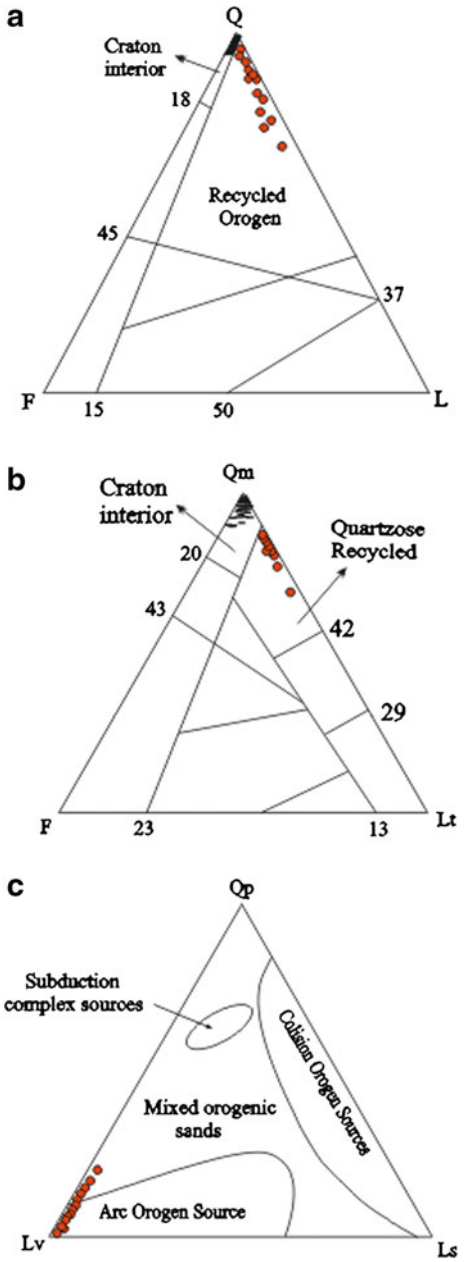

Fig. 7 Petrotectonic diagrams for analyzed Pab sandstones (after [3,4]). **a** QFL plot for detrital modes of sandstones; *crosses* indicate a Craton Interior source for both the CKsb and most of the SKsb fill, whereas *red dots*, representing samples from the upper part of the Pab Formation in the SKsb, show Recycled Orogen sources; **b** Qm-F-Lt plot for detrital modes of Pab sandstones, showing Craton Interior and Quartzose Recycled Orogen provenance. *Crosses* represent samples lacking volcanic clasts in both the CKsb and SKsb; *red dots* are samples from the upper parts of the SKsb, showing their Quartzose Recycled Orogen source; **c** Qp-Lv-Ls plot for sandstones from upper horizons in SKsb showing mainly volcanic Arc Orogen source

iments [40]. The ICV values of our Pab mudstones range between 0.075 and 0.44 (mean = 0.23; Table 4).

A–CN–K plots can also assist in determination of the composition of original source rocks [21]. This plot helps in identification of compositional variations in mudstones (as well as sandstones) caused by a variety of processes, e.g. chemical weathering, transportation, diagenesis, metamorphism and source-rock composition [41]. From our analyses, mudstones of the Pab Formation fall near the A end member in the A–CN–K plot (Fig. 8b), which is consistent with sediment that has been produced through severe chemical weathering.

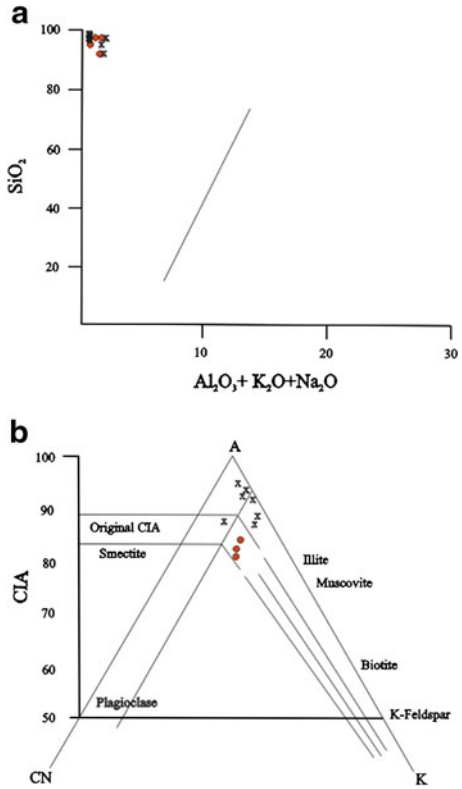

Fig. 8 **a** SiO_2–$Al_2O_3 + K_2O + Na_2O$ diagram (after [26]) for Pab Formation sandstones: *crosses* represent samples from the CKsb; *red dots* denote samples from the SKsb; **b** The A–CN–K diagram and associated CIA values (after [19]) for Pab mudstone samples; note the high CIA values for CKsb samples (*crosses*), compared to mudstones from the SKsb (*red dots*)

The CIA, calculated as shown below, is used to assess the weathering level of source rocks [19]:

$$\mathrm{CIA} = (\mathrm{Al_2O_3}/\ \mathrm{Al_2O_3} + \mathrm{CaO} + \mathrm{K_2O} + \mathrm{Na_2O}) \times 100$$

The range of the measured CIA indices in the Pab mudstones is 80.31–96.16, with a mean value of 89.05 (Table 4). Such values are indicative of severe chemical weathering and the abundance of compositionally mature alumina in the minerals [19].

The Chemical Index of Weathering (CIW) is defined as follows [19]:

$$\mathrm{CIW} = \mathrm{Al_2O_3}/\mathrm{Al_2O_3} + \mathrm{CaO} + \mathrm{Na_2O}$$

The low K_2O/Al_2O_3 ratios, high CIA (88.31–96.16) and CIW (88.76–99.49) ranges of the mudstone samples studied (Table 4) strongly suggest that most of the reduction of

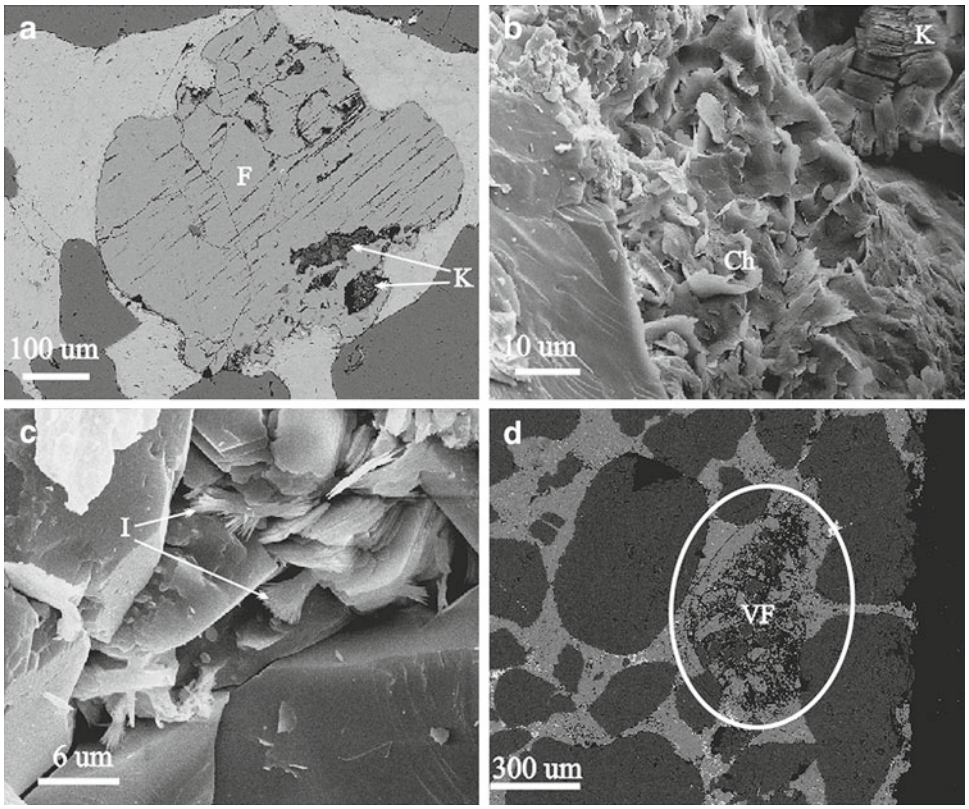

Fig. 9 SEM images of Pab Formation sandstones: **a** partial alteration of K-feldspar (**f**) to kaolinite (**k**); **b** Chlorite (*Ch*) and kaolinite (*K*) in sandstone pore-space; **c** Illite crystals (*I*) in pore-space between well-rounded grains; **d** Volcanic clast ("VF", *circled*) displaying felted texture in cement-rich sandstone

feldspar content seen in the Pab sediments occurred in the source regime, while the CIA and CIW values also confirm that the Pab muds were produced through intense chemical weathering.

In summary, the quartz-rich, mineralogically and texturally mature, composition of the Pab Formation sandstones is considered to result from tropical conditions that prevailed on the Indian craton during the latest Mesozoic [12], causing severe chemical weathering. Under these conditions, less stable minerals, such as feldspar, were effectively eliminated from the Pab detritus prior to and during transport to the Kirthar basins. Moreover, the warm and humid conditions in the source area [42], leading to intense chemical weathering of feldspar and other minerals, are further confirmed by the CIA, ICV, A–CN–K plots and the K_2O_3/Al_2O_3 ratios (Fig. 8b; Table 4).

3.4 The Nature and Significance of Pab Diagenesis

The Pab sandstones display ample evidence of relatively intense diagenetic processes, such as compaction, authigenesis, replacement, cementation and dissolution [24]. Previous studies have demonstrated that most of this diagenesis occurred at burial depths of about 2,743–2,916 and 2,704–3,252 m in the CKsb and SKsb, respectively [24]. Scanning electron microscope examination reveals that feldspar grains and volcanic fragments have been partially or wholly altered to clay minerals like kaolinite, chlorite and illite (Fig. 9a–c). In aggregate the content of clay minerals ranges between 0.3 and 6.6 % (Fig. 9a, b) and kaolinite is the most abundant clay mineral followed by chlorite and illite. The illite and chlorite are mainly associated with the alteration of volcanic clasts (at approx. 90–110 °C) during mesodiagenesis [43].

The high percentages of volcanic fragments found in the upper levels of the SKsb Pab provide important information about the prevailing climatic conditions, since relatively fresh basaltic clasts were supplied to basins on the Indian continental margin, despite the intense chemical weathering in the source area that is demonstrated by other mineralogical and geochemical criteria. It appears that the input of volcanic detritus at this time was not significantly affected by chemical weathering because this material was conveyed to the basin shortly after eruption of the parent lavas. In contrast, the relative paucity of fresh feldspar grains is interpreted to be the result of relatively low initial availability of feldspar in the source regime (due to intense weathering and recycling), together with subsequent (post-depositional) diagenetic alteration to clay minerals or replacement by calcite.

4 Conclusions

The Pab Formation is an important element in the geological history of the western margin of the Indo-Pakistan Plate. This

Late Cretaceous formation is the product of the first great flush of coarse clastics to be emplaced on the northern margin of this Plate since its separation from the rest of Gondwana in the early Mesozoic.

Our previous studies in the Kirthar region demonstrated that the Kirthar Pab was deposited within two contiguous troughs (the CKsb and SKsb) in the late Campanian to late Maastrichtian time interval. The Pab Formation sediments filling these troughs accumulated in different sedimentary environments and yield evidence of different sediment-transport paths. In the CKsb, the Pab sediments were formed in fluvio-deltaic and storm-influenced marine shelf settings by currents flowing mainly from E to W. In contrast, Pab sequences in the South Kirthar sub-basin are dominated by turbidite sands formed in submarine fans that were fed by gravity-driven currents flowing to N and NW.

Nevertheless, the petrographic and geochemical results reported here show that the composition of sediments transported into these two sub-basins remained broadly similar throughout most of the time-span represented in the Pab Formation. Pab arenites are characterized by textural and compositional maturity, as indicated by their uniformly high quartz contents, their well-sorted and well-rounded textures and the paucity of less stable mineral grains (such as feldspar). These attributes appear to result from a long history of sediment recycling and persistently low relief on the supplying hinterland, reflecting provenance predominantly from the metamorphic/plutonic basement and ancient sedimentary cover of the north-drifting Indian continental plate.

Moreover, geochemical parameters from the Pab sediments (high CIA values and low K_2O/Al_2O_3 ratios of mudstone samples; the SiO_2 versus $Al_2O_3 + K_2O + Na_2O$ plots of sandstones) demonstrate that warm and humid climatic conditions prevailed on the sediment-supplying Indian craton during the Maastrichtian, promoting intense chemical weathering and leading to the observed paucity of feldspar and other metastable mineral grains in the Pab sediments that were derived from this terrane.

The sudden appearance of appreciable quantities of basaltic detritus in the topmost levels of the Pab in the SKsb represents a significant, if localized, change in provenance (petrotectonically represented by an Arc Orogen component) that is here attributed to eruption of the great volume of Deccan Trap basalts during passage of the Indian Plate across the mantle hot spot that presently underlies the Reunion archipelago. The relatively fresh, unweathered condition of these volcanic clasts demonstrates that they were rapidly released from parent flows and transported into the Kirthar region, shortly after initial eruption in latest Maastrichtian times.

Acknowledgments Pakistan Science Foundation and Higher Education Commission are acknowledged for their partial financial support for field and Laboratory studies. The authors are thankful to the laboratory staff of the Department of Geoscience, Aarhus University, Denmark for their assistance in preparation of samples for SEM studies. Aleena Saeed and Abdul Nasir are also acknowledged for their work in preparing diagrams.

References

1. Jin, Z.; Li, F.; Cao, J.; Wang, S.; Yu, J.: Geochemistry of Daihai Lake sediments, Inner Mongolia, north China: implications for provenance, sedimentary sorting and catchment weathering. Geomorphology **80**, 147–163 (2006)
2. Chenarai, P.: Paleocurrent analyses of the Sua Khua Formation, Khorat Group, Nong Bua Lamphu region, NE Thailand. Arab. J. Sci. Eng. **37**, 115–120 (2012)
3. Dickinson, W.R.; Beard, L.S.; Brakenridge, G.R.; Erjavec, J.L.; Ferguson, R.C.; Inman, F.; Knepp, R.A.; Lindberg, F.A.; Ryberg, P.T.: Provenance of North American Phanerozoic sandstone in relation to tectonic setting. Geol. Soc. Am. Bull. **83**, 222–235 (1983)
4. Dickinson, W.R.: Interpreting provenance relations from detrital modes of sandstone. In: Zuffa, G.G. (ed.) Provenance of Arenites. Advanced Study Institute Series 148, pp. 333–361. Reidel, Dordrecht (1985)
5. Basilios, T.; Piper, G.P.; David J.W.; Piper, D.J.W.; Schaffer, M.: Varietal heavy mineral analysis of sediment provenance, Lower Cretaceous Scotian Basin, eastern Canada. Sediment. Geol. **237**, 150–165 (2011)
6. Stefani, C.; Fellin, M.G.; Zattin, M.; Zuffa, G.G.; Dalmonte, N.M.; Zanferrari, A.: Provenance and paleogeographic evolution in a multi-source foreland: the Cenozoic Venetian–Friulian Basin (NE Italy). J. Sediment. Res. **77**(11), 867–887 (2007)
7. Marenssi, S.A.; Net, L.I.; Santillana, S.N.: Provenance, environmental and paleogeographic controls on sandstone compositions in an incised-valley system: the Eocene La Meseta Formation, Seymour Island, Antarctica. Sediment. Geol. **150**(3), 301–321 (2002)
8. Taj, R.J.; Mesaed, A.A.: Facies Analyses and depositional environments of Ash Shumaysi Formation (Oligocene–Miocene), Makkah Quadrangle Wadi Ash Shumaysi, west central Arabian Shield, Saudi Arabia. Arab. J. Sci. Eng. **37**, 1459-1482 (2012)
9. McBride, E.F.: Diagenesis of the Maxon Sandstone (Early Cretaceous), Marathon Region, Texas: a diagenetic quartzarenite. J. Sediment. Res. **57**(1), 98–107 (1987)
10. Suttner, L.J.; Basu, A.; Mack, G.H.: Climate and origin of quartz arenites. J. Sediment. Petrol. **51**(4), 1235–1246 (1981)
11. Umazano, A.M.; Bellosi, E.S.; Visconti, G.; Jalfin, A.G.; Melchor, R.N.: Sedimentary record of a Late Cretaceous volcanic arc in central Patagonia: petrography, geochemistry and provenance of fluvial volcaniclastic deposits of the Bajo Barreal Formation, San Jorge Basin, Argentina. Cretaceous Res. **30**, 749–766 (2009)
12. Maslov, A.V.; Krupenin, M.T.; Gareeve, E.Z.: Lithological, lithochemical and geochemical indicators of Paleoclimate: evidence from Riphean of the Southern Urals. Lithol. Miner. Resour. **38**(05), 427–446 (2003)
13. Joo, Y.J.; Young II, L.; Zhiquiang, B.: Provenance of the Qingshuijian formation (late Carbonifereous), NE China: implication for tectonic processes in the northern margin of North China block. Sediment. Geol. **177**, 97–114 (2005)
14. Absar, N.; Raza, M.; Roy, M.; Naqvi, S.M.; Roy, A.K.: Composition and weathering conditions of Paleoproterozoic upper crust of Bundelkhand craton, Central India: records from geochemistry of clastic sediments of 1.9 Ga Gwalior Group. Precambrian Res. **168**(3–4), 313–329 (2009)
15. Roddaz, M.; Debat, P.; Nikiema, S.: Geochemistry of upper Birimian sediments (major and trace elements and Nd–Sr isotopes)

and implications for weathering and tectonic setting of the late Palaeoproterozoic crust. Precambrian Res. **159**, 197–211 (2007)
16. Raza, M.; Bhardwaj, V.R.; Ahmad, A.H.M.; Mondal, M.E.A.; Khan, A.; Khan, M.S.: Provenance and weathering history of Archaean Naharmagra quartzite of Aravalli craton, NW Indian shield: petrographic and geochemical evidence. Geochem. J. **44**(5), 331–345 (2010)
17. Taylor, S.R.; McLennan, S.M.: The Continental Crust: Its Composition and Evolution. Geol. Mag. **122**, 673–674 (1985)
18. Cox, R.; Lowe, D.R.; Cullers, R.L.: The influence of sediments recycling and basement composition on evolution of mudrock chemistry in the southwestern United States. Geochim. et Cosmochim Acta **59**, 2919–2940 (1995)
19. Nesbitt, H.W.; Young, G.M.: Earth Proterozoic climates and plate motion inferred from major element chemistry of lutites. Nature **299**, 715–717 (1982)
20. Suttner, L.J.; Dutta, P.K.: Alluvial sandstone composition and paleoclimate, I. Framework mineralogy. J. Sediment. Petrol. **56**(3), 329–345 (1986)
21. Nesbitt, H.W.; Young, G.M.: Prediction of some weathering trends of plutonic and volcanic rocks based on thermodynamic and kinetic consideration. Geochim. et Cosmochim Acta **48**, 1523–1534 (1984)
22. Khan, A.S.; Kelling, G.; Umar, M.; Kassi, A.M.: Depositional environments and reservoir assessment of Late Cretaceous sandstones in the south central Kirthat foldbelt. Pakistan. J. Petrol Geol. **25**, 373–406 (2002)
23. Umar, M.; Khan, A.S.; Kelling, G.; Kassi; A.M.: Depositional environments of Campanian–Maastrichtian successionss in the Kirthar Fold Belt, southwest Pakistan: tectonic influences on late Cretaceous sedimentation across the Indian Passive margin. Sediment. geol. **237**, 30–45 (2011)
24. Umar, M.; Friis, H.; Khan, A.S.; Kassi, A.M.; Kasi, A.K.: The effects of diagenesis on the reservoir characters in sandstones of the Late Cretaceous Pab Formation, Kirthar Fold Belt, southern Pakistan. J. Asian Earth Sci. **40**, 622–635 (2011)
25. Bannert, D.; Cheema, A.; Ahmad, A.; Schaffer, U.: The structural development of the Western Pakistan Fold Belt. Pakistan. Geol. J. Hannover **80**, 3–60 (1992)
26. Kassi, A.M.; Kelling, G.; Kassi, A.K.; Umar, M.; Khan, A.S.: Contrasting Late Cretaceous–Palaeocene lithostratigraphic successions across the Bibai Thrust, western Sulaiman Thrust Belt, Pakistan: their significance in deciphering the early-collisional history of the NW Indian Plate margin. J. Asian Earth Sci. **35**, 435–444 (2009)
27. Scotese, C.R.; Cahagan, L.M.; Larson, R.L.: Plate tectonic reconstructions of the Cretaceous–Cenozoic ocean basins. Tectonophysics **155**, 27–48 (1988)
28. Gnos, E.; Khan, M.; Mehmood, K.; Khan, A.S.; Shafique, N.A.; Villa I.M.: Bela oceanic lithoshere assemblage and its relation to the Reunion hotspot. Terra Nova **10**(2), 90–95 (1998)
29. Anwar, A., Fatmi, A.N., Hyderi, I.H.: Revised nomenclature and stratigraphy of Ferozabad, Alozai and Mona Jhal Groups of Balochistan (Axial Belt), Pakistan. Acta Minerol. Pak. **5**, 46–61 (1991)
30. Zuffa, G.G.: Optical analysis of arenites: influence of methodology on compositional results. In Zuffa, G.G. (ed.) Provenance of arenites. Reidel, Dordrecht, 165–189 (1985)
31. Fralick, P.W.; Kronberg, B.I.: Geochemical discrimination of clastic sedimentary rock sources. Sediment. Geol. **113**, 111–124 (1997)
32. Nesbitt, H.W.; Young, G.M.; McLennan, S.M.; Keays, R.R.: Effects of chemical weathering and sorting on the petrogenesis of siliciclastic sediments, with implications for provenance studies. J. Geol. **104**, 525–542 (1996)
33. Nesbitt, H.W.; Fedo, C.M.; Young, G.M.: Quartz and feldspar stability, steady and non-steady state weathering and petrogenesis of siliciclastic sands and muds. J. Geol. **105**, 173–191 (1997)
34. Hurowitz, J.A.; McLennan, S.M.: Geochemistry of Cambro-Ordovician sedimentary rocks of the northeastern United States: changes in sediment sources at the onset of Taconian orogenesis. Geology **113**, 571–587 (2005)
35. Anani, C.: Sandstone petrology and provenance of the Neoproterozoic Voltaian Group in the southeastern Voltaian Basin, Ghana. Sediment. Geol. **128**, 83–98 (1999)
36. Courtillot, V.; Gallet, Y.; Rocchia, R.; Féraud, G.; Robin, E.; Hofmann, C.; Bhandari, N.; Ghevariya, Z.G.: Cosmic markers, $^{40}Ar/^{39}Ar$ dating and paleomagnetism of the KT sections in the Anjar Area of the Deccan large igneous province. Earth Planet. Sci. Lett. **182**, 137–156 (2000)
37. Biswas, S.K.; Thomas, J.: Deccan traps and Indian Ocean volcanism, in Plummer, P.S. (ed.) First Indian Ocean Petroleum Seminar: Seychelles, pp. 187–209. United Nations Department of Technical Co-operation for Development, (1992)
38. Jaeger, J.J.; Courtillot, V.; Tapponier, P.: Paleontological view of the ages of the Deccan Traps, the Cretaceous/Tertiary boundary, and the India-Asia collision. Geology, **17**, 316–319 (1989)
39. Courtillot, V.; Besse, J.; Vandamme, D.; Montigny, R.; Jaeger, J.; Cappetta, H.: Deccan flood basalts at the Cretaceous/Tertiary boundary? Earth Planet. Sci. Lett. **80**(3–4), 361–374 (1986)
40. Weaver, C.E.: Clays, Muds and Shales. In: Developments in sedimentology, vol. 44, p 819. Elsevier, Amsterdam (1989)
41. Fedo, C.M.; Young, G.M.; Nesbitt, H.W.: Paleoclimate control on the composition of the Paleoproterozoic Serpent formation, Huronian Supergroup, Canada, a greenhouse to icehouse transition. Precambrian Res. **86**, 201–223 (1997)
42. Pfeilsticker, K.: Paleo-Climate. Institut fur Umveltphysik, Universitate Heidelberg, INF 229, 69120 Heidelberg (June 17, 2006). http://www.iup.uni-heidelberg.de/institut/studium/lehre/Uphysik/uphysik2/paleo_climate.pdf
43. Worden, R.H., Morad, S.: Clay Minerals in sandstones: controls on formation, distribution and evolution. Int. Assoc. Sedimentol. Spec. Publ. **34**, 3–41 (2003)